Review Article: Capturing the physiological complexity of the brain's neuro-vascular unit *in vitro*

Cite as: Biomicrofluidics **12**, 051502 (2018); https://doi.org/10.1063/1.5045126
Submitted: 17 June 2018 . Accepted: 27 September 2018 . Published Online: 16 October 2018

Hossein Heidari, and Hayden Taylor

Review Article: Capturing the physiological complexity of the brain's neuro-vascular unit *in vitro*

Hossein Heidari and Hayden Taylor[a)]
Department of Mechanical Engineering, University of California, 6159 Etcheverry Hall, Berkeley, California 94720, USA

(Received 17 June 2018; accepted 27 September 2018; published online 16 October 2018)

With the accelerating pace of brain research in recent years and the growing appreciation of the complexity of the brain and several brain-associated neurological diseases, the demand for powerful tools to enhance drug screening, diagnosis, and fundamental research is greater than ever. Highly representative models of the central nervous system (CNS) can play a critical role in meeting these needs. Unfortunately, *in vivo* animal models lack controllability, are difficult to monitor, and do not model human-specific brain behavior accurately. On the other hand, *in silico* computational models struggle to capture comprehensively the intertwined biological, chemical, electrical, and mechanical complexity of the brain. This leaves us with the promising domain of "organ-on-chip" *in vitro* models. In this review, we describe some of the most pioneering efforts in this expanding field, offering a perspective on the new possibilities as well as the limitations of each approach. We focus particularly on how the models reproduce the blood–brain barrier (BBB), which mediates mass transport to and from brain tissue. We also offer a brief commentary on strategies for evaluating the blood–brain barrier functionality of these *in vitro* models, including trans-endothelial electrical resistance (TEER), immunocytochemistry, and permeability analysis. From the early membrane-based models of the BBB that have grown into the Transwell® class of devices, to the era of microfluidic chips and a future of bio-printed tissue, we see enormous improvement in the reliability of *in vitro* models. More and more of the biological and structural complexity of the BBB is being captured by microfluidic chips, and the organ-specificity of bio-printed tissue is also significantly improved. Although we believe that the long-term solution will eventually take the form of automated and parallelized bio-printing systems, we find that valuable transport studies can already be accomplished with microfluidic platforms. *Published by AIP Publishing.*
https://doi.org/10.1063/1.5045126

I. INTRODUCTION

The human brain consists of a complex entanglement of fluidic and neuronal circuits that carry out biochemical, mechanical, and electrical signaling through highly specialized hierarchical tissue structures. These two circuitries have also proven to be integral to the progression of most neurological disease and therefore represent the most vital components of any *in vitro* model of the human brain. At the intersection of these two lies the blood–brain barrier (BBB), which separates the vasculature from the cerebral tissue and is central to any mass transport between the two. The critical role of the BBB means that advances in modelling it could have a huge impact on the accuracy and completeness of brain studies.

The BBB has a complex multi-layered structure. The brain vasculature's endothelial cell lining differs considerably from that of the vasculature elsewhere in the human body: in the BBB, the endothelial cells are more tightly connected by intercellular *tight junction* (TJ) proteins.[1,2]

[a)]hkt@berkeley.edu

Surrounding the endothelial layer and partially covering it are *pericytes*. Pericytes are contractile cells that provide the required structural support and vasodynamic functionality to the brain capillaries.[3] A 30–40 nm thick *basement membrane* of extracellular matrix (ECM), composed mostly of collagen type IV, laminin, and fibronectin, is wrapped around the endothelium and pericytes and is covered from the other side with glial cell foot processes such as astrocytes and neurons.[4,5] Together, this cellular structure provides low permeability compared to normal vasculature, protecting the brain from infection and, to some extent, from perturbations of chemical concentrations (Na^+, K^+, Ca^{2+}, etc.[5]).

Degradation and disruption of the BBB has been associated with the development of diseases such as cancer, multiple sclerosis, Alzheimer's disease, and many other neuro-degenerative diseases.[6–9] On the other hand, the excessively low permeability of an intact BBB can diminish the cerebral blood flow, impair the clearance of neurotoxic molecules, and cause cerebrovascular storage disorders. A great deal of effort has therefore been invested in closely approximating BBB properties in organ-on-chip models.[10,11]

The key features that appear to determine how biologically representative an *in vitro* model is of the real cerebrovascular microenvironment are as follows:

(1) the presence of the multitude of cell types that are involved in the functionality of the barrier such as vascular endothelial cells, glial cells, and neurons;[12–15]
(2) the formation of cell–cell interactions that allow the cells to be exposed to factors secreted by other neighboring cell types such as astrocytes and pericytes;[16–18]
(3) biologically relevant mechanical properties of the substrate or the surrounding ECM;[19–22]
(4) the presence of physiologically relevant flow-induced shear stress that promotes the formation of biological structures with realistic geometries and directionality, and the appearance of abundant carriers, vesicles, and intracellular constructs such as mechano-sensors, receptors, and ion-channels;[23–26]
(5) the actual geometrical and hierarchical resemblance of the cerebral blood vessels that allows for mechanical and biochemical crosstalk between different cellular compartments, as well as some dynamic mechanical triggering of the vessel walls by surrounding cells such as pericytes. The pericytes in fact serve as cerebral blood flow regulators and are highly involved in the proper functionality of the BBB.[27–30]

Such an ideal *in vitro* model of the BBB, if obtained, can allow for a high degree of control over the surrounding micro-environment, real-time monitoring and analysis, less manual preparatory work and fewer ethical issues compared with *in vivo* models, and highly reliable results due to the ease of conducting replicate experiments. With the use of such organs-on-chip, we can look forward to the appearance of patient-specific drug screening and diagnosis models.

II. TRANSWELL® CULTURES, MICROFLUIDIC CHIPS, OR BIO-PRINTED VASCULATURE: WHAT DOES EACH OF THESE APPROACHES OFFER, AND WHAT ASPECTS ARE THEY MISSING?

A. Early *in vitro* models of the brain microvasculature

The first *in vitro* experiments that were developed to model the BBB used a rather simple setup. The immobilized artificial membrane (IAM) used a planar membrane of porous silica on which proteins were immobilized to mimic the solute retention function of the endothelium by recapitulating the lipid phase of the cell membrane.[31–33] The parallel artificial membrane (PAM) model, meanwhile, used a simple phospholipid bilayer to replicate endothelial transport properties.[34,35] Such planar configurations are now generally referred to as Transwell assays, after the porous culture membranes that are commercially available. Despite the simplicity of the IAM and PAM models, they yielded valuable results and were extensively used for several years. Their popularity arose from their ease of use, the ability to mimic a variety of biological interfaces such as the BBB and the skin through simple protein immobilization, and also, in the case of the PAM, its biodegradability and the ability to model active drug transport and efflux. However, these simple models inevitably omit many characteristics of the true BBB.

Extending this idea, static, planar endothelial and epithelial monocultures and endothelial–glial co-culture models were developed that included an entire layer of cells instead of an artificial cell membrane.[36,37] The permeable layer could now express cellular responses to transported agents. Moreover, the presence of the glial cells was found to promote the formation of gap junctions and the expression of transporter proteins such as Glut1. However, even with the astrocytes in co-culture, TJs did not form properly as evidenced by trans-endothelial electrical resistance (TEER) values that were two orders of magnitude lower and permeabilities that were orders of magnitude higher than physiological conditions.[37,38] Furthermore, phase contrast micrographs showed that endothelial layers were stacked on top of each other, a situation that may have arisen because the fluids in the culture were static and physiologically relevant shear stresses were therefore absent. Despite these drawbacks, Transwell assays remain the most widely used endothelial/epithelial model. Owing to their simplicity, convenience, and the extensive literature available on their protocols, they still serve as a valuable first-step evaluation tool for many pharmaceutical and disease studies.

In an effort to enhance the 2D membrane models and incorporate shear stress, the dynamic cone and plate model was established, in which a cultured endothelium was exposed to a steady, mechanically induced shear stress.[39,40] This model enabled the study of shear stress effects on permeability and endothelial monolayer structure. The model revealed interesting information for the first time about the effect of shear and flow regime on the barrier functionality. For instance, in the presence of flow, the shape and orientation of the ECs were no longer random, and significant changes in fluid endocytosis and platelet interaction with the barrier were observed. However, it included only endothelial cells, omitting glial cells, and the steady shearing conditions differed from the pulsatile stresses found in true vasculature.

B. Microfluidic organ-on-chip models of the BBB

The introduction of Janigro's "dynamic *in vitro* BBB" (DIV-BBB), a highly engineered device, marked a substantial step forward in the sophistication of BBB models.[41–43] This model incorporated a bundle of porous hollow fibers with diameters of a few hundred microns and made of materials such as polypropylene. These fibers could be coated with different cell types, for instance, microvascular endothelial cells and astrocytes, on either side, and shear flows comparable to those in micro-vasculature could be induced.[44] The geometrical relevance of this model enabled the study of complex phenomena such as cerebral ischemia and hypo-perfusion, which are associated with insufficient blood flow and hence oxygen supply to meet the metabolic needs of the brain.

The development of engineered BBB-like environments has been accelerated by microfluidic fabrication technology. Microfluidics offer greater physiological relevance by enabling (1) spatial control over biochemical and mechanical signaling gradients,[45] (2) ECM resemblance through the use of hydrogels within the channels and chambers,[46,47] (3) interstitial flow for the exchange of nutrients, growth factors, and pharmaceutical agents,[47] (4) the potential to induce both direct and shear stresses in and around cellular membranes,[48] and (5) the creation of multiple cell culture chambers for sophisticated co-cultures.[47–49] Next, we review several microfluidic solutions that have brought us closer to an ideal BBB model.

One of the first microfluidic BBB-specific vasculature models was Griep's "BBB-on-Chip."[50] This model included two perpendicular channels stacked one above the other and separated at the point of intersection by a 10 μm-thick microporous polycarbonate membrane. This membrane served as the cell culture surface and endothelial cells were grown on it as if in a macro-scale Transwell-type assay, except with the additional benefit that flow in the channels could induce a controlled shear stress on the endothelium. Despite the possibility of co-culture, only endothelial cells were used. The platinum electrodes embedded in the chip enabled easy TEER measurements (see Sec. III B). However, the geometry of the cultured endothelium still differed considerably from that of real tubular capillaries, and the mechanical microenvironment provided by the growth substrate and channel walls was also far stiffer than in true biological tissue.

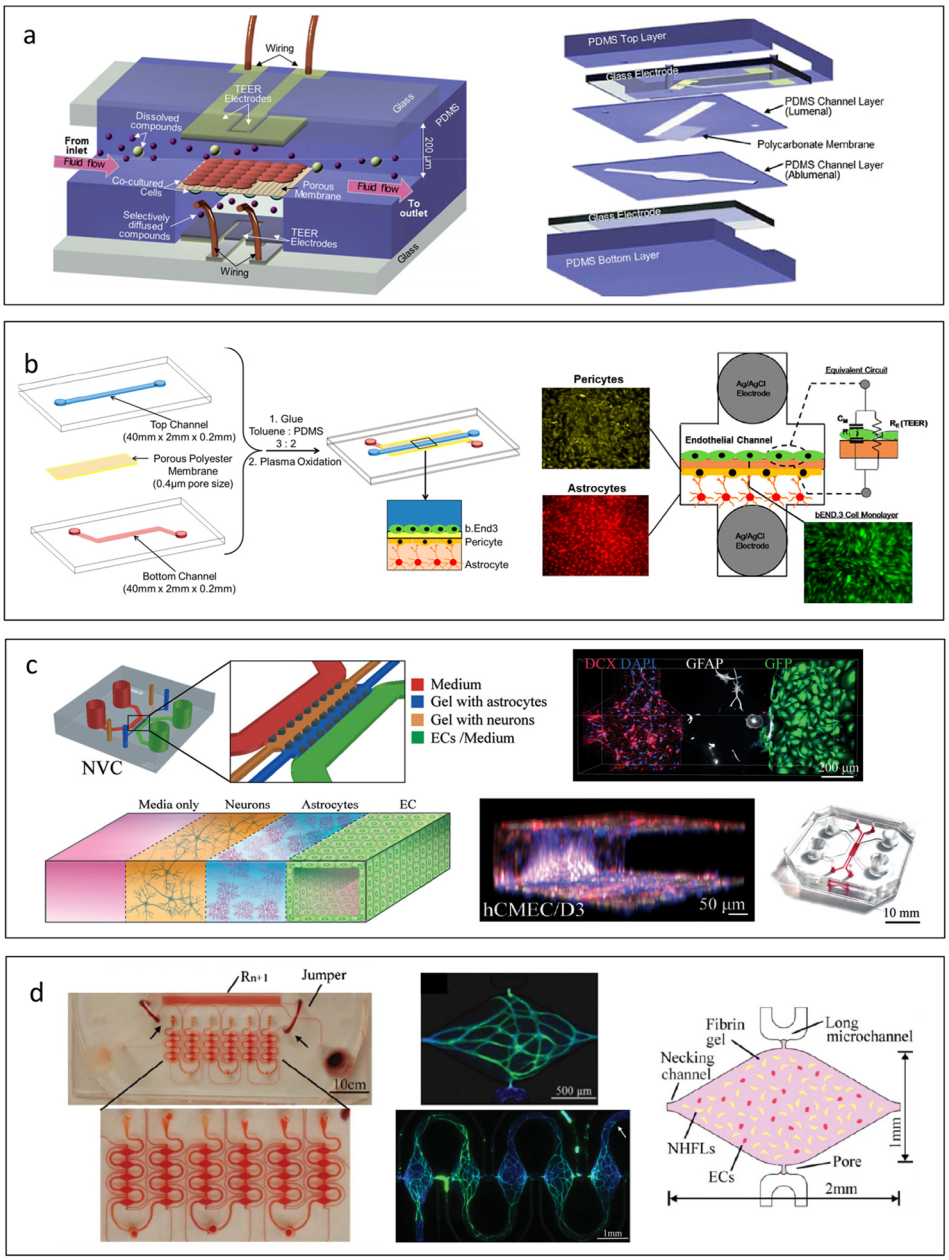

FIG. 1. Microfluidic BBB platforms based on (1) 2D porous interfaces: (a) micro-BBB model with integrated glial cell co-cultures.[51] Reproduced from *Lab on a Chip* **12**, 1784–1792 (2012) with permission of The Royal Society of Chemistry. (b) Tri-layered 3D BBB model.[52] Reproduced with permission from J. D. Wang, E.-S. Khafagy, K. Khanafer, *et al.*, "Organization of endothelial cells, pericytes, and astrocytes into a 3D microfluidic in vitro model of the blood–brain barrier," *Mol. Pharmaceutics* **13**(3), 895–906 (2016). © 2016 American Chemical Society. (2) 3D hydrogel extracellular matrices: (c) neuro-vascular chip (NVC).[56] Reproduced from *Lab on a Chip* **17**(3), 448–459 (2017) with permission of The Royal Society of Chemistry. (d) Multi-microtissue platform.[62] Reproduced from *Lab on a chip* **13**(5), 2990–2998 (2013) with permission of The Royal Society of Chemistry.

Another model that offered some additional advantages was Booth's "μBBB" [Fig. 1(a)].[51] It included a co-culture of endothelial cells (ECs) and astrocytes on opposite sides of a porous membrane similar to that in Griep's BBB-on-Chip. The setup enabled the formation of gap junctions between the astrocytes and ECs and thus higher physiological relevance than EC-only culture, as suggested by the two-fold increase in TEER values in comparison with the BBB-on-Chip. Wang *et al.* later improved the μBBB chip design by including a tri-culture of ECs, pericytes, and

astrocytes.[52] The ECs and pericytes formed a vascular bed on opposite sides of a 10 μm-thick porous membrane similar to that used in the previous work, while the astrocytes resided in the lower channel. The channel height was varied to study the effect of astrocyte–pericyte packing density on the barrier function [Fig. 1(b)]. However, the critical effect of shear stress was not considered and no visual data were provided from the achieved vascular and junctional structures.

Another way to provide a cultured 2D interface, proposed by Zervantonakis *et al.*,[53] is with a microfluidic chip consisting of multiple neighbouring and connected culture channels, one or more of which are injected with extra-cellular matrix (ECM), while the other channels are left available for media flow. The channels are separated by rows of trapezoidal pillars that direct the surface tension of an injected ECM solution to fill specific channels in a controlled way while still enabling mass transport between channels. Endothelia can be cultured on the sidewalls of the ECM at the interfaces between channels; cells can also be suspended in the ECM prior to injection. The original chip design proposed by Kamm's group has been successfully adapted to many vascular studies.[54,55] Recently, the "neuro-vascular chip" (NVC), a BBB-specific version of this design, was introduced by the same group and incorporates a co-culture of multiple cell types that are involved in the BBB [Fig. 1(c)].[56]

A similar model for the BBB that shared the idea of glial co-culture was the "Synthetic Microvasculature" model, or SyM-BBB, of Prabhakarpandian *et al.*[57] Instead of using a single-layer photolithography process followed by elastomer casting to pattern trapezoidal pillars to separate the chambers as Kamm's group did, Prabhakarpandian used two-step deep reactive ion etching (DRIE) of silicon masters to establish 3 μm-tall diffusion channels that separated the 100 μm-tall side channels from the central chamber. Whereas the larger endothelial interfaces of Zervantonakis's,[53] Adriani's,[56] and other BBB models permitted endothelial sprouting and migration, Prabhakarpandian's 3 μm-tall interface stopped cells from crossing the interface. The internal surfaces of the apical side channels hosted the endothelium and the middle chamber included glial-conditioned media. The formation of tight junctions and the activity of efflux pumps were monitored. However, TEER, shear stress, and the role of pericytes were not studied, leaving us with the question of whether the presence of co-cultured cells would influence the BBB in the same way that a dense solution of glial by-products would.

Improving on this model, Wang *et al.* demonstrated the use of a co-culture system consisting of human-induced pluripotent stem cell (iPSC)-derived brain microvascular endothelial cells and astrocytes. This 3D-printed chip not only featured a TEER measurement capability but also applied shear stress through continuous perfusion. Hence, the TEER values achieved with this model were considerably higher than with previous models and much closer to *in vivo* measurements.[58]

One of the major advantages of the 2D microfluidic designs described so far is their convenience and expected repeatability, not just from a fabrication perspective but also the practicality of microscopy both during and after the culture process. The ease of imaging planar BBB models has the potential to bring about a greater understanding of the relationship between cellular morphology, protein expression, and barrier permeability. For example, a planar BBB model positioned in a microscope's focal plane and stained for, e.g., the ZO-1 tight junction protein can reveal relevant detail of the endothelium's structure; meanwhile, the same endothelium oriented perpendicular to the focal plane during culture can be imaged to detect the transport of fluorescent dye molecules across the barrier, revealing permeability (e.g., Ref. 53). In other models, extensive use has been made of TEER as a proxy for barrier permeability. It is perhaps surprising that little work has been done to *correlate* TEER measurements—which detect the aggregate electrical behavior of an endothelium—with transport measurements of specific molecules of interest. Developing such an understanding could be an important future application of planar BBB models.

Another advantage of these 2D models over the more complex 3D designs analyzed below is their great potential for high-throughput parallelized studies. Again, this potential has not been fully realized and most of the aforementioned microfluidic chips include only a single BBB chamber. Considering these advantages, one would like to see that the 2D models improve their physiological resemblance of the BBB microenvironment. One way, as we will further explain, would be to eliminate rigid substrates from the vicinity of the cells by covering those surfaces with a thick layer of ECM gel instead of a thin coating. With the increased popularity of these soft ECM

substrates, we hope to see them as a standard feature of all 2D membrane models and microfluidic chips.

While the major microfluidic design strategies mentioned above were being developed, Bischel *et al.* introduced a technique to enable the formation of 3D vessel-like constructs within microfluidic channels and demonstrated a triple-channel chip design for the study of angiogenesis.[59,60] The technique, termed *viscous finger patterning*, worked as follows. The microfluidic channels were initially coated with fibronectin and prefilled with collagen type 1 ECM, and then a cylindrical lumen was introduced by manually pipetting media containing ECs through the channels [Fig. 2(a)]. Having three such channels side-by-side, the setup allowed the introduction of different angiogenesis factors such as vascular endothelial growth factor (VEGF) in the lateral channels. Side channels were also used to co-culture smooth muscle cells (SMCs), enabling the researchers to study their effects on the geometry and density of the endothelial sprouts extending from the central channel. This study did not report any TEER measurements: modeling the BBB was not the focus of the work. However, a few years later, Herland *et al.* used the same fabrication technique to produce a specialized BBB model.[61] In this platform, astrocytes and pericytes were

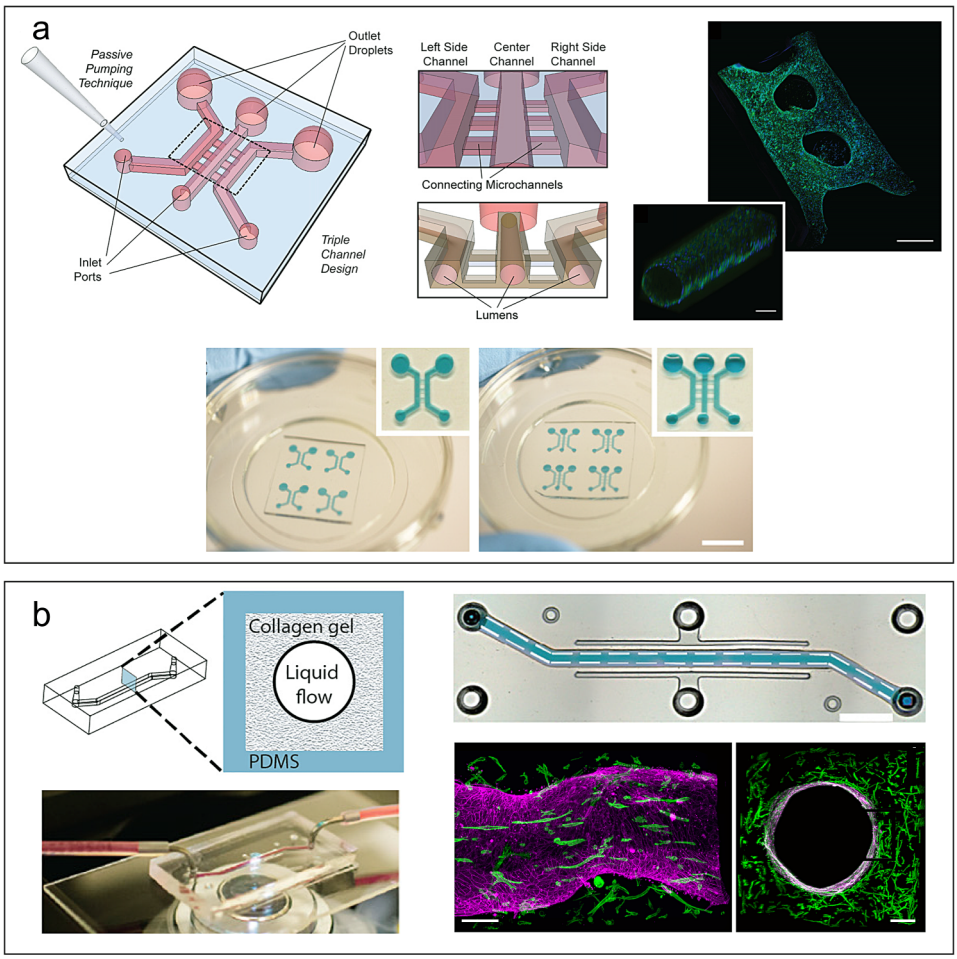

FIG. 2. Microfluidic platforms with fully 3D micro-vessels homogeneously surrounded by hydrogel extracellular matrices: (a) The triple channel angiogenesis model.[60] Reprinted from L. L. Bischel, E. W. Young, B. R. Mader, and D. J. Beebe, "Tubeless microfluidic angiogenesis assay with three-dimensional endothelial-lined microvessels," *Biomaterials* **34**(5), 1471—1477. Copyright 2013, with permission from Elsevier. (b) The 3D BBB chip with a triculture of endothelial cells, pericytes, and astrocytes.[61] A. Herland, A. D. van der Meer, E. A. FitzGerald, T.-E. Park, J. J. F. Sleeboom, and D. E. Ingber, "Distinct contributions of astrocytes and pericytes to neuroinflammation identified in a 3D human blood-brain barrier on a chip", *PLoS One* **11**(3), e0150360 (2016); used in accordance with the Creative Commons Attribution (CC BY) license.

cultured in the collagen surrounding the lumens [Fig. 2(b)], resulting in a co-culture model of the BBB with biologically relevant microenvironment properties such as stiffness.

Another distinct approach to *in vitro* modeling of vasculature is inspired by vasculogenesis and angiogenesis *in vivo* and involves the natural growth of endothelial sprouts within a 3D matrix [Fig. 1(d)]. Microvascular networks-on-a-chip fall into this category, and many groups have successfully produced perfusable endothelialized sprouts that occupy a gel chamber.[55,62,63] This method forms network geometries that appear very natural. However, naturally emergent networks do not enable multilayered cellular structures to be systematically fabricated, although bi-culture variants of such structures may conceivably emerge if another cell type is co-cultured in the surrounding matrix.[54] Moreover, the diameters of the lumens, as well as the inlet and outlet locations and the orientations of the channels, cannot be easily pre-defined. As a result, observing the diffusion of particular species through the endothelium may not be practicable.

C. Bio-fabricated and bio-printed *in vitro* vascular models

A third wave of *in vitro* vasculature models has been enabled by the emergence of additive bio-printing methods. Although these additive methods have not yet reached a level of maturity where they can reliably meet the particularly challenging requirements of BBB vasculature, their geometric flexibility, physiologically realistic mechanical properties, and scalability to larger fabrication volumes than microfluidic approaches all mean that investing effort to improve them for neurovascular modeling applications is likely to be worthwhile.

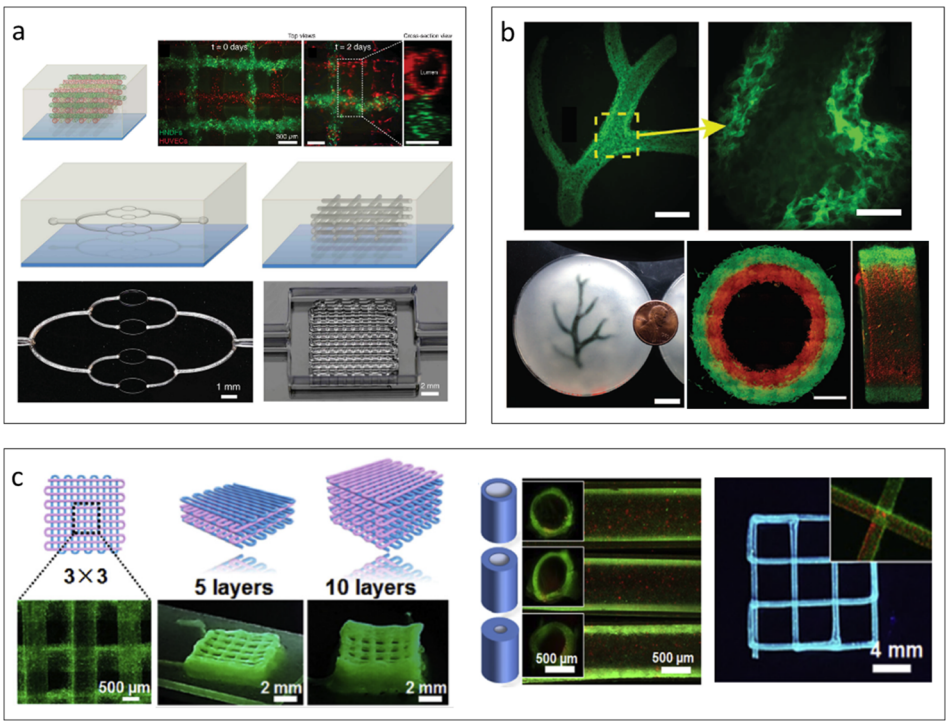

FIG. 3. Bio-fabrication strategies to produce microvascular structures: (a) 3D printed sacrificial templates.[65] Reproduced with permission from D. B. Kolesky, R. L. Truby, A. S. Gladman, T. A. Busbee, K. A. Homan, and J. A. Lewis, "3D bio-printing of vascularized, heterogeneous cell-laden tissue constructs", *Adv. Mater.* **26**, 3124–3130 (2014). © 2014 John Wiley and Sons. (b) Freeform embedding of hydrogels within a sacrificial gel (FRESH):[75] T. J. Hinton, Q. Jallerat, R. N. Palchesko, J. H. Park, M. S. Grodzicki, H.-J. Shue, M. H. Ramadan, A. R. Hudson, and A. W. Feinberg, "Three-dimensional printing of complex biological structures by freeform reversible embedding of suspended hydrogels", *Sci. Adv.* 1(9), e1500758 (2015); used in accordance with the Creative Commons Attribution (CC BY) license. (c) Direct bioprinting of perfusable networks.[71] Reprinted from W. Jia, P. S. Gungor-Ozkerim, Y. S. Zhang, K. Yue, K. Zhu, W. Liu, Q. Pi, B. Byambaa, M. R. Dokmeci, S. R. Shin, and A. Khademhosseini, "Direct 3D bioprinting of perfusable vascular constructs using a blend bioink," *Biomaterials* **106**, 58–68. Copyright 2016 with permission from Elsevier.

Bio-printing generally describes the use of a serial process such as extrusion or inkjet deposition to define three-dimensional structures in soft biocompatible polymers. In some of these processes, the soft polymer is directly deposited; in others where the soft material would be too challenging to print directly, a secondary, sacrificial, structure is generated and the biocompatible material is molded or cast around it. Rapid modeling and the creation of heterogeneous tissue structures are more easily achieved when direct ECM printing is possible.

Perhaps the simplest of the sacrificial molding techniques is the *needle removal* method. In this technique, a hydrogel is cast around a cylindrical needle, and after removing the needle, a channel remains on whose walls an endothelium can be cultured to simulate a blood vessel.[64] A geometrically generalized version of this method was introduced by Kolesky *et al.* [Fig. 3(a)] that uses a thermally gelling, aqueous material such as F127 from the Pluronic family as the sacrificial structure.[65] The key rate-limiter in such processes tends to be the liquefaction or dissolution and subsequent removal of the sacrificial material. A sacrificial casting technique does not in itself enable multilayered structures; yet, such complexity may be essential to a realistic BBB model. One solution that has been proposed by the present authors is "multi-layered micro-molding" (MμM) which combines a sequence of hydrogel casting steps to define concentric layers with differing material composition.[66] To achieve multilayered structures, MμM requires the channel networks to be molded as two halves and then bonded together, which adds an alignment step and may limit the technique to planar networks.

Meanwhile, the direct, patterned deposition of biocompatible materials has been affected in several ways. Droplet-dispensing of UV-cross-linkable polymers with inkjet technology has seen extensive use,[67–69] as has the extrusion through a nozzle of a polymer solution which subsequently gels [Fig. 3(c)].[70] In both of these approaches, cells may be suspended in the ink and so by using multiple ink channels, heterogeneous cellular structures can be defined. Sophisticated nozzle geometries have been proposed, including those that can directly print hollow cylindrical tubes of hydrogel[71] whose crosslinking may be triggered either by light or a pH change. Another strategy for building up heterogeneous structures is to culture cells inside sub-mm-diameter "tissue spheroids" and then deposit these spheroids as the building blocks of larger-scale structures.[72,73] Resolutions down to $\sim 100\,\mu$m have so far been demonstrated with all of these techniques.[74]

In cases where hollow or delicate structures are to be printed, mechanical support must usually be provided. One promising way to meet this need is "freeform embedding of hydrogels within a sacrificial gel" (FRESH), where a long extrusion needle draws out the required cellular structure within a volume of soft, thixotropic supporting gel [Fig. 3(b)].[75] However, in terms of resolution, FRESH faces exactly the same constraints as any other extrusion technique. In other words, the minimum feature size—for instance, the thickness of the vascular wall—is limited to the diameter of the extruded material. An alternative strategy to embedding the structure in support material is to entirely eliminate the use of supports through volumetric variants of optical lithography.[76,77] Although such techniques have only been introduced recently, and a bio-printing version has not emerged yet, they can hold great promise for support-free 3D printing of soft materials.

III. EVALUATING THE FUNCTIONALITY OF DIFFERENT *IN VITRO* MODELS

Here, we compare the most popular techniques for evaluating the physiological realism of a BBB model. These techniques are (a) imaging the cellular structures with selective staining, (b) measuring the trans-endothelial electrical resistance (TEER) as an indicator of endothelial permeability, and (c) time-lapse imaging of the diffusion of fluorescent molecules through the endothelium to extract permeability.

A. Visualization of tissue morphology and cellular interactions (i.e., TJs) with immunocytochemistry

Among the well-known signatures of endothelial monolayers are intercellular TJ proteins such as VE-cadherin and the zonula occludens proteins ZO-1, -2, and -3, as well as adherens junction (AJ) proteins such as α-catenin and afadin.[80,81] The TJ and AJ proteins are expressed to some

extent by epithelia and endothelia of most types, including those composed of human umbilical vein endothelial cells (HUVECs), human microvascular endothelial cells (hMECs), and human brain microvascular endothelial cells (hBMECs). The presence of these proteins indicates the formation of confluent and fenestration-free monolayers. (Fenestrations are nanometer-scale pores in the endothelial cells of some high-permeability vascular interfaces.) Stronger expression of the TJ proteins, and a higher complexity and density of the network of TJ strands binding the endothelial cells together, is associated with lower endothelial permeability[82,83] and can therefore be used as an indicator of how closely a cultured endothelium approximates the BBB. The use of ZO-1 has become widespread in microfluidic BBB models, including the BBB-on-chip,[50] the μBBB,[51] and the NVC.[56] In bio-printed platforms, on the other hand, nuclei staining and live/dead assays have been more prevalent, and there is much less information available on the inter-cellular junctions themselves and on whether bioprinted vasculatures are likely to achieve BBB-like permeabilities. This could be because very few studies have used bio-printing to produce vascular tissue *in vitro*, and almost none of these have focused specifically on the capillaries of the brain. Even strong expression of ZO-1, however, is no guarantee of physiologically realistic permeability, and so, as discussed next, measurement of actual *transport* through the endothelium is important.

B. Trans-endothelial electrical resistance (TEER) measurement

Measurement of TEER is a widespread technique for characterizing *in vitro* vascular models. Higher resistances are associated with greater confluence, or integrity, of the endothelium and with a lower permeability of the barrier.[84] There is also some evidence that TEER is correlated with how well-differentiated the endothelial cells are.[38] Reported *in vivo* values of the resistance across the BBB vary in the 1500–8000 $\Omega\,cm^2$ range;[38,85] nevertheless, a value of 150–200 $\Omega\,cm^2$ has been found to be a lower functional limit for *in vitro* models that attempt to replicate transport of certain solutes and drugs across the barrier.[86] Models with TEER in this lower-than-physiological range cannot, however, be expected to control the transport of the much smaller monatomic ions such as K^+ and Ca^{2+} which are crucial for brain function. As BBB models increasingly seek to integrate neuronal functions, considerable further advances in barrier integrity are likely to be required, and TEER can potentially be used to determine whether a cultured endothelium is adequately representative of the BBB.

TEER requires electrodes to be placed on opposite sides of the endothelium, and these are usually implemented with silver–silver chloride electrode pairs immersed in the surrounding medium or embedded into adjacent ECM.[87] Once in place, the electrodes enable constant monitoring of the TEER throughout the culture process, which may last many days. This long-term measurement capability is a distinct advantage over both cell-staining and molecular diffusion observations.

Conventional TEER measurements, however, are made at a single frequency of voltage excitation (typically around 12.5 Hz[87]) and can therefore report only a single resistance value at a given moment. Real endothelial cells and tight junctions, however, are not purely resistive but exhibit capacitive components. The use of impedance spectroscopy, involving an excitation frequency sweep, enables a richer model of the endothelial impedance to be uncovered.[87] Measurements of TEER or trans-endothelial impedance have, however, so far mostly been confined to 2D endothelium models such as the NVU,[78] the BBB-on-chip[50] and the μBBB.[51] The difficulty of threading an electrode into a cylindrical micro-capillary and the associated risk of damaging the endothelium appear to have limited the use of electrical measurements in 3D *in vitro* models (see Table I). Further innovation in fabrication techniques is needed on this front. One desirable advance would be to culture a BBB model with electrodes already in place.

C. Permeability analysis

While the electrical measurements described above may offer a convenient proxy for endothelial permeability, they do not provide specific information on a BBB model's ability to pass molecules with particular sizes and chemistries. Since the purpose of modeling the BBB is often to

TABLE I. Summary of BBB models.

Model	Category	Lumen diameter	Co-cultured cell types	Extra-cellular environment	Flow condition during culture	Characterization technique	Disease model	Ref.
PAM	Transwell-like	No lumens: 2D	Only the parallel lipid bilayer membrane	…	…	Permeability assessment for drug compounds	Passive diffusion of numerous commercial drugs	Kerns[35]
Transwell	Transwell-like	No lumens: 2D	Endothelial cells and smooth muscle cells	…	External shear using rotating disk	Limited to microscopy and visual inspection	Effect of shear on low-density lipoprotein uptake	Niwa[36]
DIV-BBB	Engineered	800 μm	Bovine aortic ECs (BAEC), C6 rat glial	Polypropylene	Dynamic flow condition → 2–4 ml/min	TEER measurements 30 days *in vitro* (DIV) $500-600\,\Omega\,\mathrm{cm}^2$		Cucullo[41]
BBB-on-Chip	Microfluidic	No lumens: 2D	Human cerebral microvascular ECs (hCMEC)	Polycarbonate membrane	Dynamic flow condition → 41.7 μl/min	TEER measurements 4 DIV 120 $\Omega\ \mathrm{cm}^2$	Effect of tumor necrosis factor alpha (TNF-α) on barrier integrity and TEER	Griep[50]
μBBB	Microfluidic	No lumens: 2D	Mouse brain ECs (bEnd3), astrocytes	Polycarbonate membrane	Dynamic flow condition → 1.3–2.6 μl/min	TEER measurements 4 DIV $250-300\ \Omega\ \mathrm{cm}^2$	…	Booth[51]
Tri-layered 3D BBB	Microfluidic	No lumens: 2D	Mouse brain ECs (BEC), mouse pericytes and astrocytes	Polyester membrane	No flow—No shear	D-Mannitol-1-^{14}C 21 DIV 182 Da $\rightarrow 5.2\times10^{-5}$ cm s^{-1} TEER measurements 21 DIV $293-318\ \Omega\ \mathrm{cm}^2$	P-glycoprotein (P-gp) efflux pump functionality	Wang[52]
Neurovascular unit (NVU)	Microfluidic	No lumens: 2D	Human brain microvascular ECs (hBMEC), pericytes, astrocytes and neurons	Collagen I (Coll I) → astrocytes, pericytes, and neurons Laminin coated polycarbonate membrane → hBMEC	Dynamic flow condition → 2.0 μl/min	TEER and Dextran 10 and 70 kDa permeabilities—data was not converted to standard literature values	Effect of glutamate on the barrier integrity and TEER	Brown[78]
Neurovascular chip (NVC)	Microfluidic	200 μm	hCMEC, astrocytes, neurons	Coll I → astrocytes and neurons polydimethylsiloxane (PDMS)/glass → hCMEC	No flow—No shear	Dextran permeability 7 DIV 10 kDa $\rightarrow 1.23\times10^{-5}$ cm s^{-1} 70 kDa $\rightarrow 3.3\times10^{-6}$ cm s^{-1}	Glutamate transport across BBB	Adriani[56]

TABLE I. (*Continued.*)

Model	Category	Lumen diameter	Co-cultured cell types	Extra-cellular environment	Flow condition during culture	Characterization technique	Disease model	Ref.
SyM-BBB	Microfluidic	No lumens: 2D	Rat BEC, astrocyte conditioned media	PDMS	Dynamic flow condition → 0.1 μl/min	Dextran 3-5 kDa permeabilities—data was not converted to standard literature values	P-gp efflux pump activity analysis	Prabhakar-pandian[57]
BBBoC	Microfluidic	No lumens: 2D	Human iPSC BMEC and astrocytes	Plastic	Dynamic flow condition → not mentioned	4-70 kDa Dextran permeability $\rightarrow 10^{-7} \sim 10^{-7}$ cm s^{-1}	Selective permeability to small molecule drugs	Wang[58]
3D BBB chip	Microfluidic	700 μm	hBMEC, pericytes, astrocytes	Collagen type I	No flow—No shear	Dextran permeability 5 DIV 3 kDa $\rightarrow 3 \times 10^{-6}$ cm s^{-1}	Effect of TNF-α on cytokine release patterns	Herland[61]
Multi microtissue platform	Microfluidic	10 μm	ECFC-EC, human fibroblasts	Fibrin gel	Dynamic flow condition → 1.1–7.1 μm/s	…	…	Hsu[62]
Needle removal	Biofabrication	200 μm	Mouse MEC, macrophages, B-cells and T-cells	Gelatin and hyaluronic acid blend hydrogel	No flow—No shear	…	Modelling immune cell and endothelial cells interactions in lymphoma	Mannino[64]
Stress induced rolling membrane (SIRM)	Biofabrication	100 μm	HUVEC, smooth muscle cells, fibroblasts	PDMS	No flow—No shear	…	…	Yuan[79]
3D printed sacrificial templates	Bioprinting	150 μm	HUVEC, fibroblasts	Gelatin methacrylate	No flow—No shear	…	…	Kolesky[65]
Direct bioprinting of perfusable networks	Bioprinting	500 μm	HUVEC, human MSC	Gelatin methacrylate, poly(ethylene glycol)-tetra-acrylate (PEGTA), alginate blend bio-ink	No flow—No shear	…	…	Jia[71]
FRESH	Bioprinting	1000 μm	Fibroblasts, myoblasts	Alginate, collagen I, fibrin gel	No flow—No shear	…	…	Hinton[75]
Microscale continuous optical bioprinting	Bioprinting	50 μm	HUVEC, mouse fibroblast, human liver cells	Gelatin methacrylate, hyaluronic acid methacrylate	No flow—No shear	…	*In vivo* implantation in mouse	Zhu[67]

study the endothelial permeability to particular toxins or candidate drugs, an awareness of molecular size-specific permeability is important. *In vitro* models have therefore made extensive use of variable molecular weight macromolecules, e.g., from the dextran family, conjugated with fluorescent dyes such as Oregon Green, Alexa Fluor, and FITC.[57] The dye source is typically introduced to one side of the endothelium, and the concentration emerging on the other side is tracked over time by optically imaging the fluorescence intensity and comparing that to the intensity observed from the known source concentration. Permeability can then be deduced from concentration changes over time.

Despite the greater specificity and accuracy of permeability studies compared with TEER, there are a few issues associated with the nature of this technique. In most of the studies that have incorporated permeability measurements, a minimum timeframe of half an hour to an hour is required to reliably capture the diffusion of species through the barrier.[57,88] Of course, this is exactly what one would expect from a functional barrier; however, it also implies that the time-to-result and responsiveness of this technique are not comparable with TEER measurements, which are instantaneous. Furthermore, as mentioned, almost all vascular models now incorporate hydrogel matrices that replicate the native structure of the endothelial basement membrane. The diffusion of the dyes into such hydrogels can be regarded as an irreversible process since it is very challenging to fully deplete the diffused fluorescent probes from inside the gel in such confined compartments. Therefore, to some extent, the technique is invasive, meaning that the samples need to be discarded after every experiment. These two constraints mean that existing permeability analysis techniques cannot be implemented as a real-time monitoring tool.

IV. HOW CLOSE ARE WE TO A RELIABLE HUMAN-SPECIFIC BBB DISEASE PLATFORM?

The integrity of the BBB, or the lack thereof, is a unique characteristic that has been linked with the genesis and progression of many diseases such as cancer, Alzheimer's, multiple sclerosis, and other neurodegenerative conditions. There is a growing appreciation that excessive increase of permeability and disruption of the BBB caused by, for example, humoral agents such as inflammatory proteins, platelet activating factors, and tumor necrosis factors[83] can diminish the cerebral blood flow,[6] impair the clearance of neurotoxic molecules, and result in cerebrovascular storage disorders such as lysosomal storage disease.[5,89] The endothelial permeability is therefore the key property that organ-on-chip models have tried to replicate. After many recent efforts to model cerebral vasculature, as summarized in Sec. II, attention is now starting to be turned to using such models as a disease platform to study the vasculature's reaction to biochemical agents including growth factors and therapeutics.

A. Cell types and the tissue microenvironment

As well as classifying BBB models from a fabrication perspective, we have compared them biologically in terms of substrate mechanics, geometry and architecture, flow conditions, and cell types. Today, BBB studies predominantly use human-specific cell lines rather than rat or mouse lines, and, moreover, the use of microvascular and even cerebral microvascular endothelial cells has been widely adopted in preference to umbilical vein or aortic endothelial cells. Additionally, several models, as discussed in Sec. II, have even incorporated co-cultures of human astrocytes and pericytes. However, along with the use of realistic cell lines comes the necessity of a proper ECM environment.

The increasing use of biocompatible hydrogels to mimic the 3D extracellular microenvironment has significantly increased the fidelity of tissue models over traditional 2D membrane-based approaches. A 3D matrix permits greater cellular mobility as well as more realistic intercellular interactions, which are crucial to cellular functionality and phenotype. 3D ECM-based models are therefore considered very useful tools for the study of, e.g., cell migration, metastasis, and angiogenesis. In the case of the NVU,[78] the NVC,[56] and the 3D BBB chip,[61] the desire for 3D culture was addressed by placing the astrocytes and pericytes in a volume of hydrogel confined

within microfluidic chambers. Nevertheless, in the first two cases, the endothelium was only partially in contact with the hydrogel. The remainder of the endothelium came into contact with the relatively stiff polymeric chamber walls, a factor that may potentially have compromised barrier integrity. In the case of the 3D BBB chip, however, the cylindrical endothelium was entirely surrounded by the collagen ECM.[61]

Collagen, a readily available ECM material, is not fully representative of brain ECM and much effort has been focused on developing ECM compositions that can better mimic human brain tissue. Human fibronectin coatings and hyaluronic acid-based hydrogels have now been combined with more conventional ECM materials, and new hybrid bio-inks are regularly introduced.[90] Hence, it is increasingly important to have a fabrication platform that can deploy a diverse range of hydrogel materials.

B. The brain side of the model

We have discussed extensively the characterization of the endothelium, whose properties are, of course, critical to any BBB model. Attention also needs to be paid to the cellular composition of the brain side of the BBB. Although many of the models discussed in Sec. II included glial cells, there has been little effort to stimulate or monitor their electrical signaling and understand how it might be affected by vasculature properties.[91–93] There has, however, been extensive recent progress in the *in vitro* modeling of stand-alone neuronal cultures, which could valuably be integrated with BBB modeling.

The introduction of multi-electrode arrays (MEAs) has advanced neuroscience by enabling individual firings of a neural circuit to be monitored *in vitro*.[94–96] For instance, a coupled microfluidic–MEA system was designed by Kanagasabapathi *et al.* to study the dynamic interactions between two different types of neurons—cortical and thalamic—under the influence of neuroactive receptor proteins.[97,98] The microfluidic design used two 8 mm-long channels with interconnecting diffusion capillaries through which the neuronal dendrites were able to extend. This channel configuration was mounted on to a 60-electrode MEA and neuron-conditioned media was added. Signal initiation and propagation from one side channel to the other was analyzed in the presence of various biochemical factors at different locations. Such platforms enable studies of the effect of a specific biochemical factor on local neuron firing, at a spatial resolution that would likely be impossible *in vivo*.

One notable effort to integrate neuronal culture and expand spatial electrical stimulation and monitoring to the third dimension while having a 3D network of microfluidic channels is found in the work of Rowe *et al.*[99] In this work, a series of micromachining processes were used to pattern structural SU-8 photoresist layers hosting a thin metal layer and sandwiching an intermediate layer of sacrificial material; upon the removal of which, hollow channels would emerge. Patterning both horizontal and vertical channels resulted in a 3D array of channels and electrodes. Although Rowe's fabrication method did not incorporate actual vasculature, it may provide a basis for doing so in the future.

Another method that has been widely used to quantify the activity levels of neurons is calcium imaging. This technique relies on imaging the fluorescence of indicator molecules which bind to Ca^{2+} and does not require the integration of electrodes. It may therefore provide a simpler route to spatially resolved observations of neuronal behavior inside a BBB model.

C. Achievements in utilizing BBB platforms for disease models

The wealth of recent innovation in fabricating *in vitro* BBB models (Table I) has begun to enable studies of the BBB's response to altered biochemical and physical conditions. For example, macrophages and several other cell types including neurons are able to signal the endothelial cells and stimulate them by secreting cytokines such as tumor necrosis factor alpha (TNF-α).[50,61] The result of this stimulation is increased endothelial permeability and tumor cell intravasation.[54] The BBB-on-chip[50] and the 3D BBB chip[61] evaluated the performance and integrity of the BBB in the presence of TNF-α through TEER measurements and cytokine release profiles, respectively. The

effects of neurotransmitters have also been studied in a few of the models.[56,78] The effects of glutamate and cold shock on barrier integrity and neural activity and function were studied in the NVU[78] and NVC[56] chips, respectively.

P-glycoprotein (P-gp) is a very important protein pertaining to the cell membrane that is in charge of pumping many foreign substances out of the cell. Hence, the activity and level of expression of this protein has been used as a quantitative measure of the functionality of the barrier in the tri-layered BBB model[52] and the SyM-BBB model.[57] In order to evaluate the activity of this efflux pump, one has to analyze the bidirectional (apical-to-basolateral and basolateral-to-apical) transport of a particular molecule that is selectively rejected by P-gp; hence, the experimental approach is very similar to permeability analysis.

The work summarized in this section represents the most sophisticated reported applications of BBB models to the study of biological function. We have so far been unable to identify an example of a BBB model applied to a specialized disease model. There are, of course, many microfluidic platforms that model only the brain tissue, in the form of single-cell analysis chips,[100] 3D neuro-spheroids,[101] and neural chips,[102] and many of those have been applied to the study of disease. However, they do not model the entire neuro-vascular interface and hence fall out of the scope of the present review.

Most of these brain-on-chip models in fact already have a mechanism of perfusion to feed the neuro-spheroids and cellular colonies. This embedded design feature could easily be improved into an endothelialized interface using the many different strategies presented here. Therefore, we hope to see the incorporation of vascular modules in these brain-on-chips. Similarly, we expect to see more in-depth studies of the neural side of the BBB, neural differentiation, synaptic function and dysfunction, and cellular signaling using the BBB platforms presented here.

V. CONCLUSIONS

There have been significant recent advances in the level of biological relevance of *in vitro* neurovascular models. There has been a clear evolution from early artificial membranes to multiplexed 3D BBB chips and NVC platforms. Important improvements have been made with respect to both the tissue microenvironment and the cell types that are used and the physiological components that have been integrated, such as flow-induced shear stress and external biochemical stimuli. Geometry and architecture have also improved significantly from the original 2D membrane models. However, despite the convenience offered by 3D methods such as viscous finger patterning, the established 2D porous polymeric membranes are still widely used and it will take some time before they are replaced by hydrogel-based 3D models.

Another possible approach that is currently being explored by several research groups is the possibility to use bio-printing to print not only the ECM scaffold but also the entire cellular construct of the vasculature. It is noteworthy that while microfluidic approaches are typically capable of producing micro-vessels in the range of 10–100 μm, state-of-the-art bio-printing techniques can only reliably produce vessels down to 100–1000 μm. This resolution barrier is likely to be overcome with the advent of new techniques and enhanced versions of prior technologies; however, for now, it remains a barrier to printing capillary-scale blood vessels. Finally, the lack of biological studies of brain-associated disease using these proposed platforms represents a huge untapped opportunity. As the biological fidelity of these models further improves, more and more attention will be drawn to their potential capabilities.

[1]N. J. Abbott, J. Anat. **200**, 629–638 (2002).
[2]N. J. Abbott, E. U. Khan, C. M. Rollinson, A. Reichel, D. Janigro, S. M. Dombrowski, M. S. Dobbie, and D. J. Begley, Novartis Found. Symp. **243**, 38–47 (2002).
[3]P. Ballabh, A. Braun, and M. Nedergaard, Neurobiol. Dis. **16**, 1–13 (2004).
[4]W. A. Banks, M. Tschöp, S. M. Robinson, and M. L. Heiman, J. Pharmacol. Exp. Ther. **302**(2), 822–827 (2002).
[5]B. T. Hawkins and T. P. Davis, Pharmacol. Rev. **57**, 173–185 (2005).
[6]N. J. Abbott, Cell Mol. Neurobiol. **25**, 5–23 (2005).
[7]S. D. Kramer, Y. B. Schutz, H. Wunderli-Allenspach, N. J. Abbott, and D. J. Begley, In Vitro Cell Dev. Biol. Anim. **38**, 566–571 (2002).

[8]S. M. Dombrowski, S. Y. Desai, M. Marroni, L. Cucullo, K. Goodrich, W. Bingaman, and M. R. Mayberg, Epilepsia **42**, 1501–1506 (2001).
[9]C. M. Liberto, P. J. Albrecht, L. M. Herx, V. W. Yong, and S. W. Levison, J. Neurochem. **89**, 1092–1100 (2004).
[10]D. Malonek, U. Dirnagl, U. Lindauer, K. Yamada, I. Kanno, and A. Grinvald, Proc. Natl. Acad. Sci. U.S.A. **94**, 14826–14831 (1997).
[11]K. R. Lee, N. Kawai, S. Kim, O. Sagher, and J. T. Hoff, J. Neurosurg. **86**, 272–278 (1997).
[12]N. J. Abbott, A. A. Patabendige, D. E. Dolman, S. R. Yusof, and D. J. Begley, Neurobiol. Dis. **37**, 13–25 (2010).
[13]S. F. Zhou, L. L. Wang, Y. M. Di, C. C. Xue, W. Duan, C. G. Li, and Y. Li, Curr. Med. Chem. **15**, 1981–2039 (2008).
[14]M. Marroni, N. Marchi, L. Cucullo, N. J. Abbott, K. Signorelli, and D. Janigro, Curr. Drug. Targets **4**, 297–304 (2003).
[15]H. Wolburg and A. Lippoldt, Vascul. Pharmacol. **38**, 323–337 (2002).
[16]N. J. Abbott, L. Ronnback, and E. Hansson, Nat. Rev. Neurosci. **7**, 41–53 (2006).
[17]Y. Igarashi, H. Utsumi, H. Chiba, Y. Yamada-Sasamori, H. Tobioka, Y. Kamimura, K. Furuuchi, Y. Kokai, T. Nakagawa, M. Mori and N. Sawada, Biochem. Biophys. Res. Commun. **261**(1), 108–112 (1999).
[18]U. Tontsch and H. C. Bauer, Brain Res. **539**(2), 247–253 (1991).
[19]C. Hartmann, A. Zozulya, J. Wegener, and H. J. Galla, Exp. Cell Res. **313**, 1318–1325 (2007).
[20]I. J. Fidler, Semin. Cancer Biol. **21**, 107–112 (2011).
[21]H. Wolburg, S. Noell, A. Mack, K. Wolburg-Buchholz, and P. Fallier-Becker, Cell Tissue Res. **335**, 75–96 (2009).
[22]T. L. Sellaro, A. K. Ravindra, D. B. Stolz, and S. F. Badylak, Tissue Eng. **13**, 2301–2310 (2007).
[23]J. A. Frangos, S. G. Eskin, L. V. McIntire, and C. L. Ives, Science **227**(4693), 1477–1479 (1985).
[24]S. P. Olesen, D. Claphamt, and P. Davies, Nature **331**(6152), 168–170 (1988).
[25]D. E. Conway, M. T. Breckenridge, E. Hinde, E. Gratton, C. S. Chen, and M. A. Schwartz, Curr. Biol. **23**(11), 1024–1030 (2013).
[26]Y. S. J. Li, J. H. Haga, and S. Chien, J. Biomech. **38**(10), 1949–1971 (2005).
[27]C. N. Hall, C. Reynell, B. Gesslein, N. B. Hamilton, A. Mishra, B. A. Sutherland, F. M. O'Farrell, A. M. Buchan, M. Lauritzen, and D. Attwell, Nature **508**, 55–60 (2014).
[28]C. M. Peppiatt, C. Howarth, P. Mobbs, and D. Attwell, Nature **443**, 700–704 (2006).
[29]T. L. Pallone and E. P. Silldorff, Nephron Exp. Nephrol. **9**, 165–170 (2001).
[30]A. Armulik, G. Genové, M. Mäe, M. H. Nisancioglu, E. Wallgard, C. Niaudet, L. He, J. Norlin, P. Lindblom, K. Strittmatter, B. R. Johansson, and C. Betsholtz, Nature **468**, 557–561 (2010).
[31]A. Reichel and D. J. Begley, Pharm. Res. **15**, 1270–1274 (1998).
[32]M. Kansy, F. Senner, and K. Gubernator, J. Med. Chem. **41**(7), 1007–1010 (1998).
[33]C. Y. Yang, S. J. Cai, H. Liu, and C. Pidgeon, Adv. Drug Deliv. Rev. **23**(1), 229–256 (1997).
[34]E. H. Kerns, L. Di, S. Petusky, M. Farris, R. Ley, and P. Jupp, J. Pharm. Sci. **93**(6), 1440–1453 (2004).
[35]L. Di, E. H. Kerns, K. Fan, O. J. McConnell, and G. T. Carter, Eur. J. Med. Chem. **38**(3), 223–232 (2003).
[36]K. Niwa, T. Kado, J. Sakai, and T. Karino, Ann. Biomed. Eng. **32**(4), 537–543 (2004).
[37]S. Santaguida, D. Janigro, M. Hossain, E. Oby, E. Rapp, and L. Cucullo, Brain Res. **1109**(1), 1–13 (2006).
[38]A. Wolff, M. Antfolk, B. Brodin, and M. Tenje, J. Pharm. Sci. **104**(9), 2727–2746 (2015).
[39]C. F. Dewey Jr., S. R. Bussolari, M. A. Gimbrone Jr., and P. F. Davies, J. Biomech. Eng. **103**, 177–185 (1981).
[40]S. R. Bussolari, C. F. Dewey Jr., and M. A. Gimbrone Jr., Rev. Sci. Instrum. **53**, 1851–1854 (1982).
[41]L. Cucullo, M. S. McAllister, K. Kight, L. Krizanac-Bengez, M. Marroni, M. R. Mayberg, K. A. Stanness, and D. Janigro, Brain Res. **951**, 243–254 (2002).
[42]K. A. Stanness, E. Guatteo, and D. Janigro, Neurotoxicology **17**, 481–496 (1996), PubMed ID 8856743.
[43]K. A. Stanness, L. E. Westrum, E. Fornaciari, P. Mascagni, J. A. Nelson, S. G. Stenglein, T. Myers, and D. Janigro, Brain Res. **771**, 329–342 (1997).
[44]L. Cucullo, P. O. Couraud, B. Weksler, I. A. Romero, M. Hossain, E. Rapp, and D. Janigro, J. Cereb. Blood Flow. Metab. **28**, 312–328 (2008).
[45]M. H. Wu, S. B. Huang, and G. B. Lee, Lab Chip **10**, 939–956 (2010).
[46]I. Meyvantsson and D. J. Beebe, Annu. Rev. Anal. Chem. **1**, 423–449 (2008).
[47]E. W. Young and D. J. Beebe, Chem. Soc. Rev. **39**, 1036–1048 (2010).
[48]D. Huh, G. A. Hamilton, and D. E. Ingber, Trends Biol. **21**, 745–754 (2011).
[49]K. J. Regehr, M. Domenech, J. T. Koepsel, K. C. Carver, S. J. Ellison-Zelski, W. L. Murphy, L. A. Schuler, E. T. Alarid, and D. J. Beebe, Lab Chip **9**, 2132–2139 (2009).
[50]L. M. Griep, F. Wolbers, B. De Wagenaar, P. M. Ter Braak, B. B. Weksler, I. A. Romero, P. O. Couraud, I. Vermes, A. D. van der Meer, and A. Van den Berg, Biomed. Microdevices **15**, 145–150 (2013).
[51]R. Booth and H. Kim, Lab Chip **12**, 1784–1792 (2012).
[52]J. D. Wang, E. S. Khafagy, K. M. Khanafer, S. Takayama, and M. E. El-Sayed, Mol. Pharm. **13**(3), 895–906 (2016).
[53]I. K. Zervantonakis, S. K. Hughes-Alford, J. L. Charest, J. S. Condeelis, F. B. Gertler, and R. D. Kamm, Proc. Natl. Acad. Sci. U.S.A. **109**(34), 13515–13520 (2012).
[54]J. S. Jeon, S. Bersini, M. Gilardi, G. Dubini, J. L. Charest, M. Moretti, and R. D. Kamm, Proc. Natl. Acad. Sci. U.S.A. **112**(1), 214–219 (2015).
[55]Y. Shin, J. S. Jeon, S. Han, G. S. Jung, S. Shin, S. H. Lee, R. Sudo, R. D. Kamm, and S. Chung, Lab Chip **11**(13), 2175–2181 (2011).
[56]G. Adriani, D. Ma, A. Pavesi, R. D. Kamm, and E. L. Goh, Lab Chip **17**(3), 448–459 (2017).
[57]B. Prabhakarpandian, M. C. Shen, J. B. Nichols, I. R. Mills, M. Sidoryk-Wegrzynowicz, M. Aschner, and K. Pant, Lab Chip **13**, 1093–1101 (2013).
[58]Y. I. Wang, H. E. Abaci, and M. L. Shuler, "Microfluidic blood–brain barrier model provides in vivo-like barrier properties for drug permeability screening," Biotechnol. Bioeng. **114**(1), 184–194 (2017).
[59]L. L. Bischel, S. H. Lee, and D. J. Beebe, J. Lab. Automation **17**, 96–103 (2012).
[60]L. L. Bischel, E. W. Young, B. R. Mader, and D. J. Beebe, Biomaterials **34**, 1471–1477 (2013).
[61]A. Herland, A. D. van der Meer, E. A. FitzGerald, T. E. Park, J. J. Sleeboom, and D. E. Ingber, PLoS One **11**(3), e0150360 (2016).

[62]Y. H. Hsu, M. L. Moya, C. C. Hughes, S. C. George, and A. P. Lee, Lab Chip **13**(5), 2990–2998 (2013).
[63]J. E. Leslie-Barbick, J. J. Moon, and J. L. West, J. Biomater. Sci. Polym. Ed. **20**(12), 1763–1779 (2009).
[64]R. G. Mannino, A. N. Santiago-Miranda, P. Pradhan, Y. Qiu, J. C. Mejias, S. S. Neelapu, and W. A. Lam, Lab Chip **17**(3), 407–414 (2017).
[65]D. B. Kolesky, R. L. Truby, A. Gladman, T. A. Busbee, K. A. Homan, and J. A. Lewis, Adv. Mater. **26**, 3124–3130 (2014).
[66]H. Heidari and H. Taylor, preprint bioRxiv 242156, 2018.
[67]W. Zhu, X. Qu, J. Zhu, X. Ma, S. Patel, J. Liu, P. Wang, C. S. Lai, M. Gou, Y. Xu, K. Zhang, and S. Chen, Biomaterials **124**, 106–115 (2017).
[68]T. Q. Huang, X. Qu, J. Liu, and S. Chen, Biomed. Microdevices **16**, 127–132 (2014).
[69]M. S. Hahn, L. J. Taite, J. J. Moon, M. C. Rowland, K. A. Ruffino, and J. L. West, Biomaterials **27**(12), 2519–2524 (2006).
[70]S. V. Murphy and A. Atala, Nat. Biotechnol. **32**, 773–785 (2014).
[71]W. Jia, P. S. Gungor-Ozkerim, Y. S. Zhang, K. Yue, K. Zhu, W. Liu, Q. Pi, B. Byambaa, M. R. Dokmeci, S. R. Shin and A. Khademhosseini, Biomaterials **106**, 58–68 (2016).
[72]C. Norotte, F. S. Marga, L. E. Niklason, and G. Forgacs, Biomaterials **30**, 5910–5917 (2009).
[73]K. Jakab, C. Norotte, B. Damon, F. Marga, A. Neagu, C. L. Besch-Williford, A. Kachurin, K. H. Church, H. Park, V. Mironov, R. Markwald, G. Vunjak-Novakovic, and G. Forgacs, Tissue Eng. Part A **14**, 413–421 (2008).
[74]V. Mironov, R. P. Visconti, V. Kasyanov, G. Forgacs, C. J. Drake, and R. R. Markwald, Biomaterials **30**, 2164–2174 (2009).
[75]T. J. Hinton, Q. Jallerat, R. N. Palchesko, J. H. Park, M. S. Grodzicki, H. J. Shue, M. H. Ramadan, A. R. Hudson, and A. W. Feinberg, Sci. Adv. **1**(9) (2015).
[76]M. Shusteff, A. E. Browar, B. E. Kelly, J. Henriksson, T. H. Weisgraber, R. M. Panas, N. X. Fang, and C. M. Spadaccini, Sci. Adv. **3**(12), 5496 (2017).
[77]B. Kelly, I. Bhattacharya, M. Shusteff, R. M. Panas, H. K. Taylor, and C. M. Spadaccini, preprint arXiv:1705.05893, 2017.
[78]J. A. Brown, V. Pensabene, D. A. Markov, V. Allwardt, M. D. Neely, M. Shi, C. M. Britt, O. S. Hoilett, Q. Yang, B. M. Brewer, P. C. Samson, L. J. McCawley, J. M. May, D. J. Webb, D. Li, A. B. Bowman, R. S. Reiserer, and J. P. Wikswo, Biomicrofluidics **9**(5), 054124 (2015).
[79]B. Yuan, Y. Jin, Y. Sun, D. Wang, J. Sun, Z. Wang, W. Zhang, and X. Jiang, Adv. Mater. **24**(7), 890–896 (2012).
[80]X. Jiao, P. He, Y. Li, Z. Fan, M. Si, Q. Xie, and D. Huang, Dis. Markers. **2015**, 860120.
[81]E. Steed, M. S. Balda, and K. Matter, Trends Cell Biol. **20**(3), 142–149 (2010).
[82]U. Kniesel and H. Wolburg, Cell. Mol. Neurobiol. **20**(1), 57–76 (2000).
[83]J. D. Huber, R. D. Egleton, and T. P. Davis, Trends Neurosci. **24**(12), 719–725 (2001).
[84]K. Benson, S. Cramer, and H. Galla, Fluids Barriers CNS **10**(1), 5 (2013).
[85]C. Crone and S. P. Olesen, Brain Res. **241**(1), 49–55 (1982).
[86]A. Reichel, D. J. Begley, and N. J. Abbott, in *The Blood-Brain Barrier* (Humana Press, 2003), pp. 307–324.
[87]B. Srinivasan, A. R. Kolli, M. B. Esch, H. E. Abaci, M. L. Shuler, and J. J. Hickman, J. Lab. Automation **20**(2), 107–126 (2015).
[88]S. Han, Y. Shin, H. E. Jeong, J. S. Jeon, R. D. Kamm, D. Huh, L. L. Sohn, and S. Chung, Sci. Rep. **5**, 18290 (2015).
[89]D. J. Begley, C. C. Pontikis, and M. Scarpa, "Lysosomal storage diseases and the blood-brain barrier," Curr. Pharm. Des. **14**(16), 1566–1580 (2008).
[90]S. R. Caliari and J. A. Burdick, Nat. Methods **13**(5), 405 (2016).
[91]P. Bezzi and A. Volterra, Curr. Opin. Neurobiol. **11**, 387–394 (2001).
[92]J. Lok, P. Gupta, S. Guo, W. J. Kim, M. J. Whalen, K. van Leyen, and E. H. Lo, Neurochem. Res. **32**, 2032–2045 (2007).
[93]S. Guo and E. H. Lo, Stroke **40**, S4–S7 (2009).
[94]M. E. Spira and A. Hai, Nat. Nanotechnol. **8**, 83–94 (2013).
[95]K. W. Chaudhary, C. J. Strock, J. A. Bradley, H. H. Luithardt, M. J. Cato, L. A. King, M. Cato, and D. J. Murphy, J. Pharm. Toxicol. Methods **75**, 159–160 (2015).
[96]Y. Yi, J. Park, J. Lim, C. J. Lee, and S. H. Lee, Trends Biotechnol. **33**, 762–776 (2015).
[97]T. T. Kanagasabapathi, D. Ciliberti, S. Martinoia, W. J. Wadman, and M. M. Decré, Front. Neuroeng. **4**, 13 (2011).
[98]T. T. Kanagasabapathi, M. Franco, R. A. Barone, S. Martinoia, W. J. Wadman, and M. M. Decré, J. Neurosci. Methods **214**, 1–8 (2013).
[99]L. Rowe, M. Almasri, K. Lee, N. Fogleman, G. J. Brewer, Y. Nam, B. C. Wheeler, J. Vukasinovic, A. Glezerd, and A. B. Frazier, Lab Chip **7**, 475–482 (2007).
[100]A. M. Taylor, M. Blurton-Jones, S. W. Rhee, D. H. Cribbs, C. W. Cotman, and N. L. Jeon, Nat. Methods **2**(8), 599 (2005).
[101]J. Park, B. K. Lee, G. S. Jeong, J. K. Hyun, C. J. Lee, and S. H. Lee, Lab Chip **15**(1), 141–150 (2015).
[102]A. Kunze, R. Meissner, S. Brando, and P. Renaud, Biotechnol. Bioeng. **108**(9), 2241–2245 (2011).